


RESEARCH ARTICLE

An event-based magnetoencephalography study of simulated driving: Establishing a novel paradigm to probe the dynamic interplay of executive and motor function

Elizabeth A. Walshe¹  | Timothy P. L. Roberts^{1,2,3} | Chelsea Ward McIntosh¹ |
Flaura K. Winston^{1,3,4} | Dan Romer⁵ | William Gaetz^{1,2,3}

¹Center for Injury Research and Prevention, Children's Hospital of Philadelphia, Philadelphia, Pennsylvania, USA

²Lurie Family Foundations' MEG Imaging Center, Department of Radiology, Children's Hospital of Philadelphia, Philadelphia, Pennsylvania, USA

³Department of Radiology, Perelman School of Medicine, University of Pennsylvania, Philadelphia, Pennsylvania, USA

⁴Department of Pediatrics, Perelman School of Medicine, University of Pennsylvania, Philadelphia, Pennsylvania, USA

⁵Annenberg Public Policy Center, University of Pennsylvania, Philadelphia, Pennsylvania, USA

Correspondence

William Gaetz, Lurie Family Foundations' MEG Imaging Center, Department of Radiology, Children's Hospital of Philadelphia, 34th St. and Civic Center Boulevard, Philadelphia, PA 19104, USA.
Email: gaetz@chop.edu

Funding information

National Institute of Health, Grant/Award Number: NIH-R21 5R21NS118410-02; Children's Hospital of Philadelphia (CHOP) Foerderer Award; Center for Child Injury Prevention Studies; Center for Injury Research and Prevention at CHOP; Annenberg Public Policy Center at the University of Pennsylvania

Abstract

Magnetoencephalography (MEG) is particularly well-suited to the study of human motor cortex oscillatory rhythms and motor control. However, the motor tasks studied to date are largely overly simplistic. This study describes a new approach: a novel event-based simulated drive made operational via MEG compatible driving simulator hardware, paired with differential beamformer methods to characterize the neural correlates of realistic, complex motor activity. We scanned 23 healthy individuals aged 16–23 years (mean age = 19.5, SD = 2.5; 18 males and 5 females, all right-handed) who completed a custom-built repeated trials driving scenario. MEG data were recorded with a 275-channel CTF, and a volumetric magnetic resonance imaging scan was used for MEG source localization. To validate this paradigm, we hypothesized that pedal-use would elicit expected modulation of primary motor responses beta-event-related desynchronization (B-ERD) and movement-related gamma synchrony (MRGS). To confirm the added utility of this paradigm, we hypothesized that the driving task could also probe frontal cognitive control responses (specifically, frontal midline theta [FMT]). Three of 23 participants were removed due to excess head motion (>1.5 cm/trial), confirming feasibility. Non-parametric group analysis revealed significant regions of pedal-use related B-ERD activity (at left precentral foot area, as well as bilateral superior parietal lobe: $p < .01$ corrected), MRGS (at medial precentral gyrus: $p < .01$ corrected), and FMT band activity sustained around planned braking (at bilateral superior frontal gyrus: $p < .01$ corrected). This paradigm overcomes the limits of previous efforts by allowing for characterization of the neural correlates of realistic, complex motor activity in terms of brain regions, frequency bands and their dynamic temporal interplay.

Abbreviations: B-ERD, beta event-related desynchronization; FMT, frontal midline theta; MEG, magnetoencephalography; MRGS, movement-related gamma synchrony.

This is an open access article under the terms of the [Creative Commons Attribution-NonCommercial-NoDerivs](https://creativecommons.org/licenses/by-nc-nd/4.0/) License, which permits use and distribution in any medium, provided the original work is properly cited, the use is non-commercial and no modifications or adaptations are made.

© 2023 The Authors. *Human Brain Mapping* published by Wiley Periodicals LLC.

KEYWORDS

beta event-related desynchronization, driving simulator, frontal midline theta, magnetoencephalography, motor control, movement-related gamma synchrony

1 | BACKGROUND AND SIGNIFICANCE

The neural processes underlying even simple, and certainly complex, movements demand a dynamic interplay of multiple brain regions involved in motor planning and execution. Oscillatory rhythms in the brain are thought to play a significant role in both executing and controlling movement, and magnetoencephalography (MEG), with source localization and intrinsic high temporal resolution (ms), is particularly well-suited to the noninvasive study of these cortical oscillatory rhythms (Cohen, 1972; Hämäläinen et al., 1993; for reviews see Cheyne, 2013; van Wijk et al., 2012). Advances in MEG analytical methods, such as differential beamforming, have optimized the spatial and spectral resolution of MEG and its use to investigate the spatial organization of neural oscillatory dynamics over the motor cortex (Barratt et al., 2018; Cheyne et al., 2006; Cheyne et al., 2008). These methodological developments have resulted in significant advances in knowledge regarding the association between movement-related cortical oscillations (in the beta band, 14–30 Hz, and gamma band, 60–90 Hz) and motor behavior during development, in health and in disease (Gaetz et al., 2010, 2013, 2020; Heinrichs-Graham et al., 2014; Heinrichs-Graham & Wilson, 2015, 2016; Muthukumaraswamy, 2010; Ulloa, 2022; Wilson et al., 2010; Wilson et al., 2011).

With the differential beamformer approach, trial-by-trial changes in band-limited cortical oscillation power are contrasted with resting (pretask) brain oscillatory activity, and peak changes are then localized in the brain, corresponding to changes in oscillatory power within that specific frequency band. For example, event-related desynchrony (decrease in power) in the beta band (B-ERD), relative to resting beta activity, occurs in a ~ 500 ms window around a simple button press event (Cheyne et al., 2006; Gaetz et al., 2010; Gaetz et al., 2020) and has been long used as an index of primary motor function, serving as a presurgical identifier of motor cortex location. Similarly, movement-related gamma band synchronization (MRGS) can also index cortical motor activity closely tied to discrete movements of the body, typically occurring briefly (~200 ms) around movement onset (Cheyne et al., 2008; Gaetz et al., 2010, 2011; Muthukumaraswamy, 2010; Pfurtscheller et al., 2003; Wilson et al., 2010). This MRGS has been shown to be part of a movement-related gamma network that is sensitive to more complex motor control and other higher cognitive processes during movement execution. For example, MRGS amplitude and peak frequency is modulated by cognitive-motor response interference (Gaetz et al., 2013; Heinrichs-Graham et al., 2018; Wiesman et al., 2020), MRGS amplitude is reduced when there is increased contextual response certainty (Wiesman et al., 2021). Thus, the spatial, spectral, and temporal sensitivity of MEG provides us a valuable set of tools to investigate the neural correlates of motor control and execution in laboratory-based motor tasks.

One challenge in the field is that the motor tasks typically studied using MEG tend to lack the complexity and ecological relevance of

everyday motor behaviors, whereby increased higher-level cognitive processes are needed for dynamic motor control in response to a changing environment. Indeed, for most studies of motor cortex activity, the conventional experimental approach is to elicit a simple repeatable movement from the research participant (or clinical patient), such as a visually cued button-press response or a self-paced “ballistic” movement of an isolated body part (e.g., individual finger movements), critically interleaved with a “rest” period for each trial. While this approach has produced valuable information about movement-related cortical oscillations generally (e.g., how beta rhythms change with typical development and differ in attention deficit hyperactivity disorder [ADHD] and autism spectrum disorder [ASD] populations, etc., see Heinrichs-Graham et al., 2018; and Gaetz et al., 2020), it may limit the focus to corticospinal outflow neural responses (e.g., indexing primary motor cortex activity), with limited insight to the array of “non-primary” parieto-frontal networks responsible for planning and coordinating complex movements more relevant in the real-world. On tasks with greater motor control demands (e.g., bimanual movements, visuo-motor integration, and increased executive control), we anticipate that more complex cortical processes will emerge (Battaglia-Mayer et al., 2003; Wenderoth et al., 2006).

In this proof-of-concept MEG study, we use an ecologically relevant event-marked prototypical simulated-driving task combined with frequency-specific differential beamformer spatial-filter methods to probe primary motor function as well as higher-order cognitive control over performance. Driving is a ubiquitous and high-risk, universally-relevant skill that relies on integrated sensory, motor, and cognitive function (Anstey et al., 2005, 2012; Apolinario et al., 2009) (for example, to operate the vehicle, respond to visual cues, maintain attention, and avoid hazards in real time). Even relatively simple aspects of driving, such as responding to traffic light changes, steering and speed control nonetheless require access to these integrated neural processes. For example, stopping in response to a red-light cue at an upcoming intersection not only requires the physical movement for brake pedal depression, but also situational awareness (Baumann & Krems, 2007) for the prolonged and coordinated planning and execution of braking (e.g., monitoring of speed and spatial positioning during controlled deceleration in order to stop at the appropriate target location).

Previous neuroimaging studies (typically using electroencephalography [EEG], functional magnetic resonance imaging [fMRI], or functional near-infrared spectroscopy [fNIRS]) have attempted to measure neural activity during simulated and on-road driving tasks, within the field of traffic safety research (Calhoun et al., 2002; Kan et al., 2013; Balters et al., 2017; Schier, 2000; and for reviews, see: Balters et al., 2021; Calhoun & Pearson, 2012; Haghani et al., 2021). A recent review (Haghani et al., 2021) highlights that neuroimaging studies to date have largely focused on studying intoxicated driving (e.g., see Calhoun et al., 2004; Calhoun & Pearson, 2012), distracted driving

(with a secondary task) (Fort et al., 2010; Schweizer et al., 2013; Xu et al., 2017; Yuen et al., 2021), and fatigue and drowsiness detection (Gharagozlou et al., 2015; Zhao et al., 2012; for a review, see Li & Chung, 2022). Also, few simulated driving studies have included ecological driving tasks that require control of a steering wheel and pedals, rather than watching a video of driving or using a joystick or button box controller (Spiers & Maguire, 2007; Walter et al., 2001). Despite the clear potential advantages in spectral, temporal, and spatial resolution, very few studies to date have utilized MEG imaging (Fort et al., 2010; Sakihara et al., 2014). While one MEG study (Fort et al., 2010) indeed adopted an event-related design, analogous to that which we describe, that study focused on attentional demands and distracted driving, and used only broadband (0–75 Hz, and thus, not frequency-specific measurements) and did not report on either beta or gamma band motor cortical activity, nor any index of cognitive control. On the other hand, the other MEG study by Sakihara et al. (Sakihara et al., 2014) using differential beamformer spatial filter analysis identified the existence and location of frontal midline theta (FMT; 3–9 Hz) band, an established marker of cognitive control/executive function (Cavanagh & Frank, 2014), but collapsed all activity over time, essentially integrating over the whole driving experience (3 min), and thus not resolving its temporal dynamics and its interplay with motor cortex activity.

The current study builds on these two prior studies by: (i) adopting an event-related approach, analogous to Fort et al., but focusing on the motor and motor control systems, and (ii) using a frequency-specific analysis, like Sakihara et al., allowing separation of theta, beta, and gamma oscillations. This approach affords harnessing the full merit of MEG—that is a spatial, temporal, and spectral characterization of brain function during simulated driving. Thus, in this study, we adopted an event-related approach, containing embedded and time-stamped events corresponding to traffic light changes as well as driver behavior (e.g., acceleration and braking). Drivers performed the same prototypical simulated driving task repeated over numerous trials so that we could assess time-locked changes in cortical oscillation power associated with specific aspects of driving behavior. This approach then uses frequency-specific differential beamformer-based spatial-filter analysis of specific events that occur while driving (e.g., onset of accelerator and brake pedals). We examined movement-related cortical oscillations in a group of 23 typically developing teens and young adults (limited to adolescents and young adults to (1) reduce variability in driving experience, and (2) reduce variability due to significant endogenous differences in participant oscillatory power which is known to change with age: see Gaetz et al., 2010; Rossiter et al., 2014; Wilson et al., 2010).

The primary objective of the current study is to determine whether well-characterized lab-based measures of motor cortex neural oscillatory activity (e.g., B-ERD and MRGS) can also be identified in a complex and ecologically valid setting, simulated driving, or whether the ongoing cognitive demands of such a paradigm might obscure these indices (that have hitherto been primarily observed using simple, button-press paradigms of limited generalizability). Recapitulation of these well-described observations (i.e., ground truth physiological responses) of motor cortex activity in this novel, complex, and

ecologically valid paradigm would support the further development of this paradigm scenario and methodological approach. Second, anticipating the spatial identification of nodal activity in the motor control network, including B-ERD and MRGS in primary motor cortex [MI] and FMT activity, as has been previously reported, we hypothesize that the high temporal resolution of MEG, combined with our event-related paradigm, will allow resolution of the temporal dynamics of interplay of activity in these regions subserving complex behavior.

2 | MATERIALS AND METHODS

2.1 | Participants

This study recruited 23 typically developing individuals (sex = 18 males and 5 females; mean age = 19.4, SD = 2.4, range = 16–24 years) through email campaigns and posted study flyers. All participants provided informed consent (or assent with parental consent) and in compliance with the Declaration of Helsinki. Eligible participants were 16 years or older and spoke English as a first language. Exclusion criteria included: previous diagnosis of ASD, Asperger's syndrome, pervasive developmental delay, other psychiatric disorders, seizure and neurologic disorders, severe claustrophobia, or uncorrectable hearing or vision issues. Twenty participants had their full license, and three participants were still in the learner's permit status. Three subjects with excessive head motion or large movement artifacts across numerous trials during the study were excluded, leaving $N = 20$ in the final analytical sample, all of which were right-handed.

2.2 | Procedures

All study procedures were approved by the CHOP Institutional Review Board. Participants completed an MEG brain scan while seated upright and using the MEG-compatible driving simulator hardware (Current Designs, Inc., <https://www.curdes.com>). Participants were acclimated to the driving simulation (Diagnostic Driving, Inc., <https://diagnosticdriving.com>) using an introductory scenario to get used to the steering wheel/pedals and practice trials for the driving scenario (detailed below). Once familiarized with the vehicle controls and scene, participants then completed the experimental drive trials. Following this, participants were offered a break before proceeding to complete an approximately 1-hour magnetic resonance imaging (MRI) brain scan for anatomic localization of MEG detected brain activity, through source modeling.

2.3 | Driving simulation

2.3.1 | Driving simulation hardware

The hardware for driving simulation consisted of a MEG-compatible projection screen paired with an MEG-compatible driving simulator

package (Current Designs, Inc.) including a steering wheel, brake, and accelerator pedal. Light is sent from an interface unit (outside the shielded room) through a long optical fiber bundle to sensors on the driving control hardware: see Figure 1. These sensors modulate the light in proportion to movement (e.g., depressing the brake pedal, etc.) and this light signal is transmitted back to the interface unit where the detected signals are converted into standard USB control signals for use with the driving simulation software. In addition, these signals are also sent to the MEG ADC interface unit as voltage traces proportional to steering, accelerator and brake pedal activity for recording synchronized with MEG data acquisition. These traces are inspected for events of interest (such as evidence of onset of braking or acceleration) and indicated by manually-placed data markers off-line. The Current Designs hardware interfaces with Diagnostic Driving Inc. software which delivers custom-built driving scenarios for this study (developed in the unity3d programming environment), described in detail below.

2.3.2 | Driving simulation task paradigm

We custom-built a prototypical driving scenario with only basic driving task demands for accelerating, coasting and braking, in order to facilitate identifying the landmark physiological responses of the motor cortex time-locked to driving movements (accelerating and braking) without additional cognitive demands (as with ambient traffic, pedestrians, hazards, etc.). Starting with a basic drive allows for future studies to systematically increase complexity within the driving scene for a more challenging driving scenario. Thus, this drive required starting and stopping on cue at traffic light intersections on a straight roadway (speed management), with no turns, and no other vehicles or pedestrians (see Figure 2). The paradigm begins with a rest period (9 s) during which the drivers were instructed to look at the rest screen (with only the word “rest” projected on screen) and relax their hands and feet away from the vehicle controls. After rest, the simulated scene begins with the driver’s vehicle in a stopped position at a



FIGURE 1 Image of driver using simulated driving set-up in the magnetoecephalography laboratory

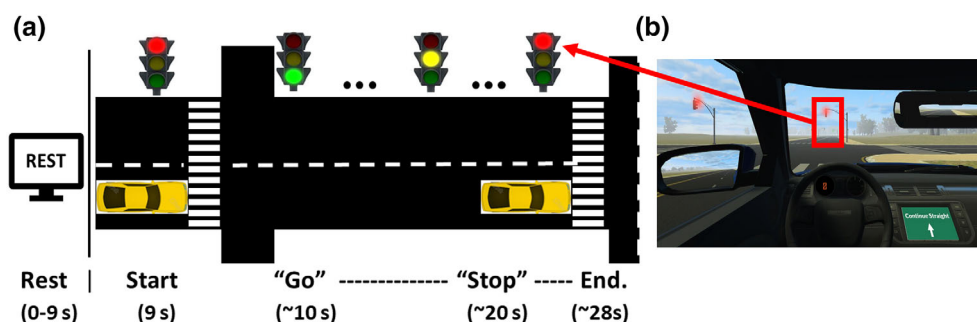


FIGURE 2 Schematic illustration of the driving trials including: (a) an aerial-view schematic illustration of the rest period and trial sequence of the driving task, with (b) a snapshot of the driving scene on screen as the driver approaches the red-light intersection at the end of the trial. Each subject was given the following instructions: The driving task involves starting and stopping at traffic light intersections. “Please wait for the light to turn green to ‘go’ and be sure to ‘stop’ close to the thick solid white lines at the next red light. Otherwise, please keep your speed at 35 miles per hour.”

red traffic-light intersection on a simple straight roadway with no other vehicles present. After 1 s, the red light turns green, signaling participants to start accelerating, with the dashboard navigation screen indicating they should drive straight forward. As they approach the next traffic-light intersection, the green light ahead turns to yellow, and then red, signaling to the participant to brake and stop at the upcoming intersection. Once the driver comes to a complete stop (at the intersection), the rest screen appears for the next trial starting with a rest period.

All participants were given an opportunity to practice driving in a simple driving scene on a simple roadway without other vehicles or pedestrians. Basic motor movements of driving were performed: (i) accelerating (using accelerator pedal), (ii) braking (using brake pedal), and (iii) practice steering on curved sections of the road. A limited set of practice trials were conducted to allow participants to become familiar with the task and vehicle controls (i.e., steering wheel and pedal sensitivity). For the experimental drive, there was a block of 20 repeated trials consisting of a rest period (9 s) at the beginning, followed by active driving (~19 s). The trial duration of the simulated drive depends largely on how fast the car travelled per trial. Drivers were asked to accelerate and maintain a speed of ~35 mph, thus the total of 20 trials took approximately 530 s (a maximum of 30 s per trial \times 20 trials, thus 600 s maximum). Maximum speed and trial duration, as well as accelerator pedal and brake pedal onset timepoints, were recorded as behavioral indices of performance.

Just out of view, on the border of the driving scene projection, a photodiode is placed over a black/white voxel that displays luminance changes built into the driving simulation software presentation as event triggers for the MEG data, for example, marking when each rest period ended and when the traffic lights changed color. These markers were used for defining the event/cue-related epochs for MEG analysis. Mean values for each cue-response latency were noted and mean accelerator pedal and brake pedal onset times are plotted along with the percent oscillatory power change versus time for each of the frequency bands of interest (beta [B-ERD], gamma [MRGS], and theta [FMT]).

2.4 | MEG data acquisition

Whole-head MEG recordings were conducted using a CTF-Omega 275 channel system (CTF MEG International Services, Coquitlam, B.C.) sampled continuously at 600 Hz (continuous recording of 600 s duration [0–150 Hz band-pass] containing repeated “trials”). MEG data was acquired while participants sat upright and viewed the driving scene back-projected (via mirrors) to a screen ~90 cm in front of the seat (controlled via a simulation presentation computer outside the magnetically shielded room). Prior to data acquisition, three actively driven head localization fiducial coils were placed at the nasion and preauricular locations and used for co-registration of the digitized head surface with the subject's brain anatomical MRI. Head position was continuously monitored at 10 Hz throughout each MEG recording.

2.5 | MRI acquisition

Whole-brain MRI was conducted using a 3.0 Tesla Siemens Verio™ MR scanner using a 32-channel receive-only head coil. We obtained a 3D magnetization prepared rapid acquisition gradient-echo (MPRAGE) scan in axial orientation, with field of view = $256 \times 256 \times 192 \text{ mm}^3$ and matrix = $256 \times 256 \times 192 \text{ mm}^3$ to yield 1 mm isotropic voxel resolution (TR/TE = 1900/2.87 ms; inversion time = 1100 ms; flip angle = 9 degrees). MRI-visible markers were placed at the three MEG fiducial coil locations for co-registration with the MEG data.

2.6 | MEG analysis

As mentioned above, the goal is to assess movement-related cortical oscillations associated with specific movements occurring on each trial. Thus, the continuously recorded data were epoched into trials of 28 s duration, starting with the onset of the 9 s rest condition. First, maximum head motion was noted for each individual in our sample ($N = 20$), and 7 trials out of a possible 395 total trials were removed due to head motion in excess of 1.5 cm. Third-order gradient correction was applied, and direct current (DC) offset removed using the CTF analysis program DataEditor; version 5.4.1. Accelerator and brake pedal onset times were then marked manually for each trial.

2.6.1 | Beamformer analysis

The synthetic aperture magnetometry (SAM) beamformer algorithm was used for source localization (Gaetz et al., 2010; Vrba & Robinson, 2001). For each subject, noise-normalized differential power values were calculated (integrated across a spectro-temporal “active” window compared to a “baseline” time windows) at the spatial source location of each individual's peak responses and expressed as the pseudo- t statistic, hereafter abbreviated as “pseudo- t ” (Nichols & Holmes, 2002). Using SAM, we first explored two frequency bands where we hypothesized modulations of motor cortical oscillations associated with the accelerator and brake pedal onsets (B-ERD and MRGS). To establish the timing details of our experimental approach, B-ERD (14–30 Hz), and MRGS (60–90 Hz) precise baseline and active window times and durations were established from visual inspection of the time-frequency responses (TFRs). Specifically, B-ERD differential source activity was assessed using a 5 s active window (–1.0 to 4.0 s) with respect to brake onset time, contrasted to a 5 s baseline period time-referenced to the “Rest” period (3–8 s). MRGS was assessed using a 3 s active window (–1 to 2 s) with respect to brake onset and contrasted with a 3 s (5–8 s) baseline “Rest” period. The previous MEG study by Sakihara et al. (2014) reported FMT band responses during simulated driving. Thus, we also explored whether we would observe event-specific synchrony in FMT (3–9 Hz). We used a 4 s active window (time locked to pedal onset) contrasted with a 4 s baseline time window (4–8 s), again following a visual assessment of FMT responses from time-frequency data.

2.6.2 | MEG group analysis

Magnetic resonance imaging structural images and the individual differential SAM beamformer results B-ERD, MRGS, and FMT analysis were first normalized to the Montreal Neurologic Institute (MNI) template using a nonlinear (FNIRT) (Andersson et al., 2008) registration transform. Voxelwise general linear modeling was applied to the normalized beamformer images using permutation-based nonparametric testing, correcting for multiple comparisons using the FMRIB Software Library (FSL: <http://www.fmrib.ox.ac.uk/fsl/>). That is, nonparametric permutations (Nichols and Holmes, 2002) for each frequency band (one sample) *t*-tests were conducted using the full permutation set (4096) for each band with 10 mm of variance smoothing following previously published MEG/beamformer methods (Hamandi et al., 2011). Family-wise error corrected *p*-values are reported using a nonparametric null distribution of the maximum (omnibus) voxel-wise test statistic.

2.6.3 | Region of interest time–frequency analysis

Time-frequency responses for peak B-ERD, MRGS, and FMT locations were evaluated by first noting the peak source location of the SAM localized response per individual. Peak locations for each frequency band of interest were then used for “virtual sensor” TFR analysis using the Hilbert transform. TFR analyses of source waveforms for each individual's peak source locations were conducted at 0.5 Hz frequency steps between 1 and 100 Hz and represented as a percentage change from baseline for each frequency band of interest, and then averaged over subjects. Percent change in B-ERD, MRGS, and FMT frequency bands was then assessed and plotted over time in relation to the mean time of accelerator and brake pedal onset.

2.7 | Statistical analysis

The frequency bands selected for source analysis were also used for statistical inference. For each frequency band, statistical inference was done for a selected set of time windows (indicated below in each analysis) using a nonparametric permutation test to correct for multiple comparisons. Pearson's product–moment correlation analysis was used to calculate the association between frequency bands and age, as well as driving performance. To address the multiple tests performed, we applied a conservative Bonferroni corrected *p*-value threshold ($p < .0167$ to accommodate the three frequency bands) to infer statistical significance. Given observed changes in behavioral performance over trials, we conducted a post hoc analysis of changes in frequency power over trials also. We examined this by comparing the first and second half of trials across the experiment (given the small sample size and thus inadequate subject-to-noise ratio for more granular analysis).

3 | RESULTS

Of the 20 participants remaining in this study (sex = 16 males, 4 females; mean age = 19.6; SD = 2.5; range = 16–24), average head motion was 0.57 cm overall (SD = 0.27 cm; range = 0.22–1.37 cm). The average number of trials available for analysis after head motion correction was 19.5 (SD = 1.28; range = 15–20).

On average, accelerator pedal onset in response to the green traffic light occurred at 10.3 s (SD = 0.4) after the start of the trial, with time zero set to the onset of the 9 s rest period. Average brake onset time was 19.9 s (SD = 1.0), which varied more across participants, as evidenced by the increased SD. The mean trial duration for the group was 25.0 s, with a statistically significant reduction in trial duration over trials: trial duration was 0.7 s shorter in the latter half of trials versus the first half of trials (25.4 vs. 24.7 s, $t[17] = -4.05$, $p = .0008$). However, the mean max speed (39.2 mph across all trials) did not differ between early and late trials (38.6 mph in early trials versus 39.2 mph; paired *t*-test: $t[15]$, $p = .14$). Neither max speed nor trial duration were associated with age, but both of these behavioral performance measures were highly correlated with each other. For this reason, only trial duration was selected for use in subsequent analysis (as a more complete index of driving performance, e.g., reflecting the integrated contributions of faster acceleration, speed, and braking, all of which are subject to modulation through learning, familiarity and/or habituation).

3.1 | Beta event-related desynchrony

Nonparametric group analysis revealed significant regions of B-ERD activity, localized to the left precentral neuroanatomically-expected “foot area”, as well as bilateral superior parietal lobe ($p < .01$ corrected): see Figure 3. Time-frequency plots of source waveform activity obtained from the peak spatial locations showed that B-ERD duration was approximately 200–300 ms starting around the time of accelerator pedal onset (which was less variable across participants) and approximately 1000 ms around the time of brake onset (which was more variable across participants). Average B-ERD power had a significant positive, but weak, association with age ($R^2 = 0.23$, $p = .033$), that did not survive Bonferroni correction, but nonetheless represents support for a hypothesis relating B-ERD with age.

3.2 | Movement related gamma synchrony

Nonparametric group analysis revealed significant regions of MRGS, localized to the medial precentral gyrus, consistent with contralateral midline “foot area” ($p < .01$ corrected): see Figure 4. Time-frequency plots of source waveform activity obtained from each subject's peak location showed MRGS lasting approximately 200 ms starting around the onset of accelerator pedal depression and approximately 300 ms around braking. Although the transition to red traffic light was preceded by a yellow traffic light, visual inspection of the behavioral

FIGURE 3 Grand averaged ($N = 20$) beta frequency (14–30 Hz) over trial time (a), power change over trial time (b), and peak locations (c), demonstrating beta event-related desynchrony (Beta-ERD) around accelerator (“gas”) and brake pedal use. The $p < .01$ threshold for significant peak locations (c) is derived from the nonparametric permutation testing and used as a mask. Displayed within the masked region are the true average pseudo- t statistics from the actual study. Thus, all pseudo- t 's in that region (within the mask) meet a criterion of $p < .01$, but the average intensity of these resultant maps reveal the underlying group average value of each parameter in pseudo- t units.

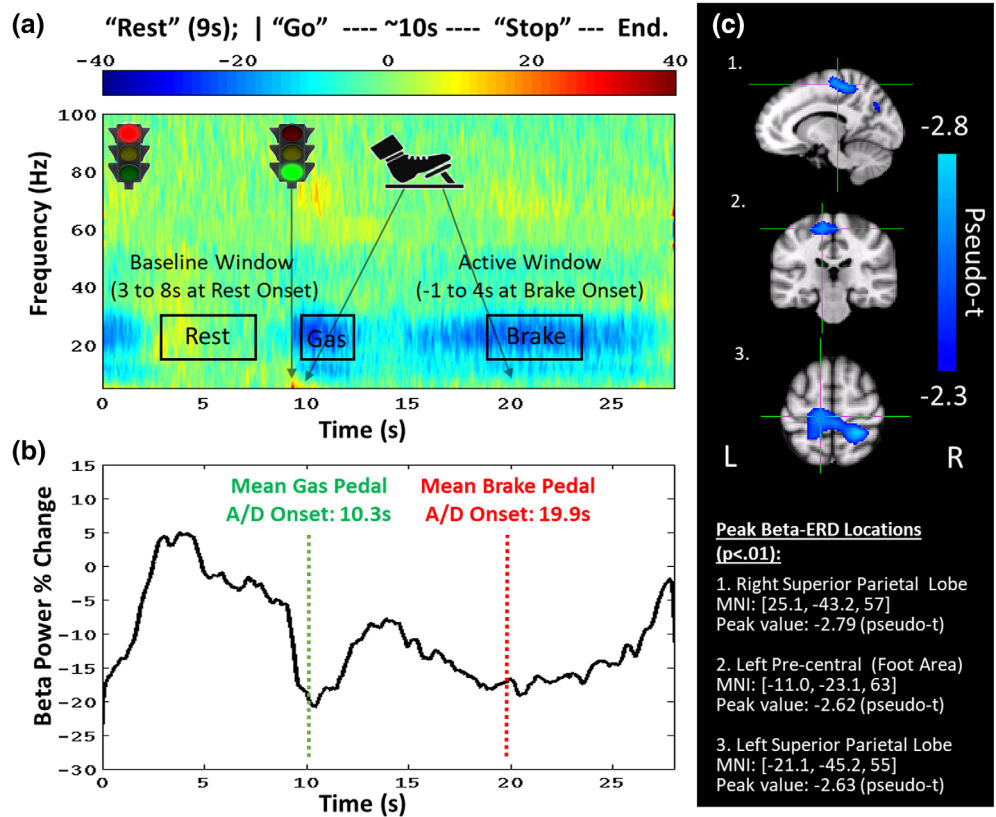
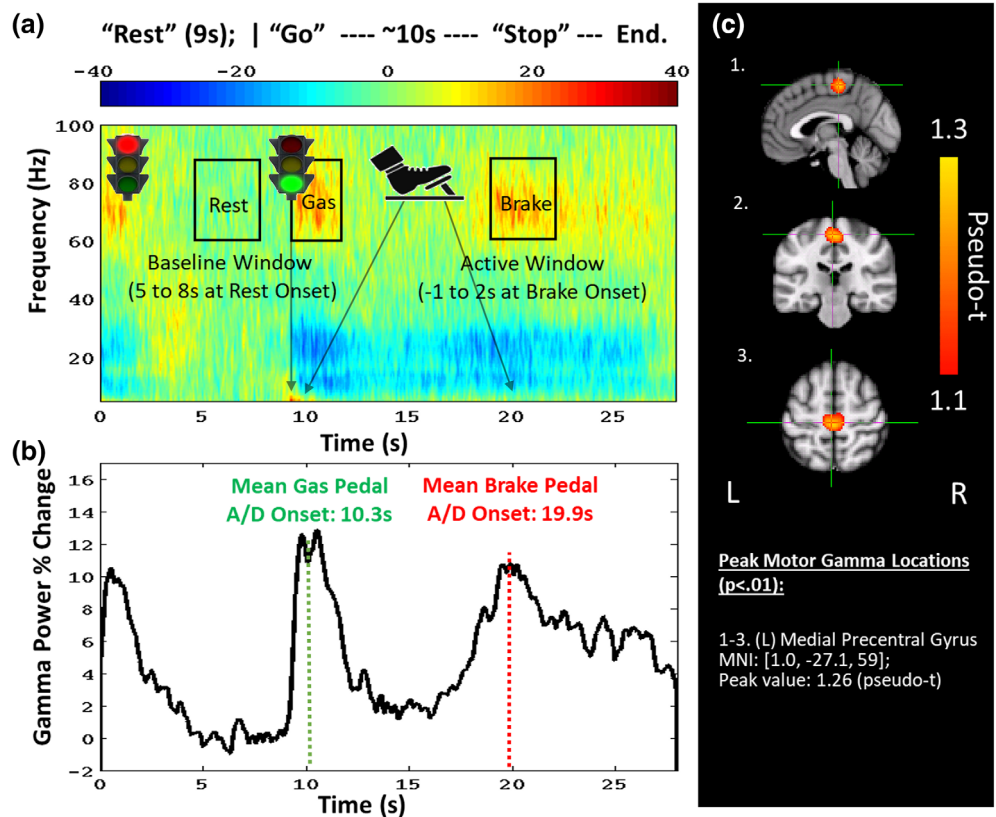


FIGURE 4 Grand averaged ($N = 20$) motor gamma related synchrony (MRGS) frequency over trial time (a), power change over trial time (b), and peak locations (c), demonstrating MRGS at the onset of the accelerator (“gas”) pedal and similarly around brake pedal use. The $p < .01$ threshold for significant peak locations (c) is derived from the nonparametric permutation testing and used as a mask. Displayed within the masked region are the true average pseudo- t statistics from the actual study. Thus, all pseudo- t 's in that region (within the mask) meet a criterion of $p < .01$, but the average intensity of these resultant maps reveal the underlying group average value of each parameter in pseudo- t units.



responses did not, in any case, indicate a coordinated motor response until after red-light onset. MRGS power appeared to increase with age, but there was no statistically significant association.

Furthermore, MRGS power appeared to decrease across trials. In a post hoc analysis, we examined if changes in MRGS power were associated with the observed decrease in trial duration over trials. The

mean MRGS peak value was reduced from 1.68 (SEM = 0.17) in the first half of trials, to 1.26 (SEM = 0.17) in the second half of trials: this

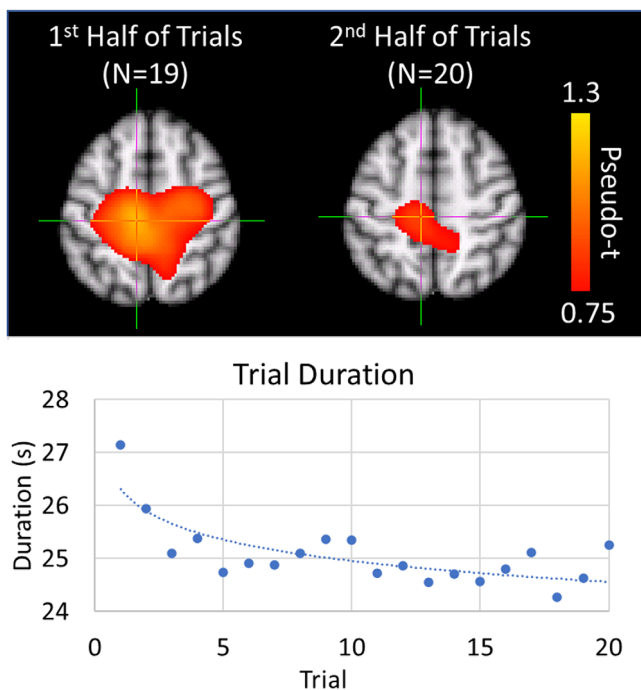


FIGURE 5 Changes in grand averaged movement-related gamma synchrony power between 1st and 2nd half of trials (top of figure), and trial duration in seconds plotted over trials (bottom of figure)

difference was significant at the corrected p value ($p = .011$). However, after excluding one extremely outlying MRGS value (beyond the 99% confidence interval) in the early trial condition, this difference was only statistically significant at the uncorrected p-value: $p = .028$. See Figure 5. However, MRGS did correlate with overall trial duration ($R^2 = 0.16$, $p = .015$) with a decrease of 0.19 units of gamma power per second reduction in trial duration.

3.3 | Frontal midline theta synchrony

Nonparametric group analysis revealed significant regions of FMT band activity, specifically at the left and right superior frontal gyri ($p < .01$ corrected): See Figure 6. Time-frequency analysis based on peak FMT activity showed a significant increase in theta power at both the onset of accelerator and brake pedal depression in the driving task. However, this theta activity was sustained for a longer duration after the onset of braking (see Figure 6). A nonsignificant trend in FMT power increase with age was observed. FMT power appeared to be associated with pedal onset time, so we conducted a post hoc multiple regression analysis, considering the potential association between behavioral pedal onset time and candidate explanatory regressors age and FMT power. There was no association between FMT and age ($F = 0.65$, $p = .43$), but a significant negative association between accelerator pedal onset time and FMT power at brake onset ($F = 10.2$, $p = .005$) with a slope of -0.40 such that accelerator onset time was faster by 0.4 s per unit increase in brake-related FMT (range

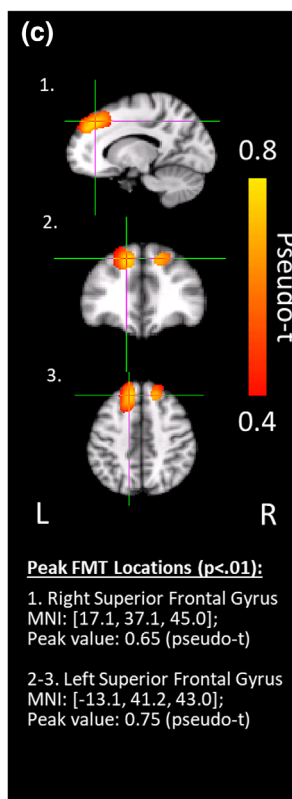
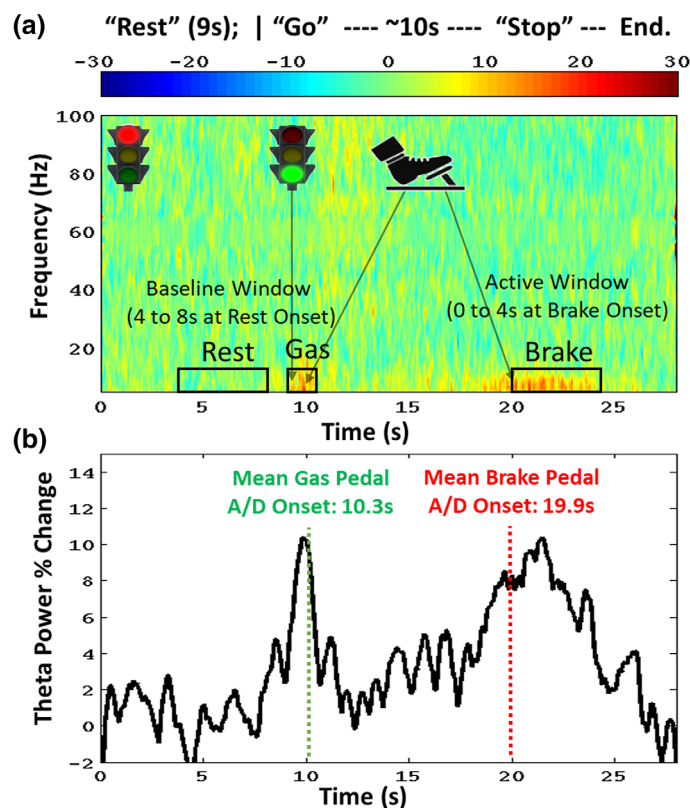


FIGURE 6 Grand averaged frontal midline theta (FMT) frequency over trial time (a), power change over trial time (b), and peak locations (c), demonstrating FMT synchrony at the onset of the accelerator (“gas”) pedal and similarly around brake pedal use. The $p < .01$ threshold for significant peak locations (c) is derived from the nonparametric permutation testing and used as a mask. Displayed within the masked region are the true average pseudo-t statistics from the actual study. Thus, all pseudo-t’s in that region (within the mask) meet a criterion of $p < .01$, but the average intensity of these resultant maps reveal the underlying group average value of each parameter in pseudo-t units.

of FMT powers was 0.7–3.3 pseudo-*t*). Thus, it seems the expression of FMT signaling is significantly associated with faster behavioral responses for accelerator pedal onset.

4 | DISCUSSION

This study aimed to establish a novel paradigm for the field by combining MEG and frequency-specific differential beamformer methods with an event-based simulated driving scenario. The main findings of this study are the observation of primary motor and higher-level motor control neural oscillatory activity, in different spatial nodes, in different frequency bands and, critically, at inter-related times relative to specific events in the simulated driving scenario. We established the validity of our more complex and ecologically valid simulated driving paradigm by observing the well-characterized measures of motor cortex neural oscillatory activity, in this case, B-ERD and MRGS. In addition, we demonstrate that the high temporal and spectral resolution of MEG, combined with our event-related paradigm, allows resolution of the temporal dynamics of interplay of activity in different brain regions, with correlates to underlying behavior. Specifically, we note the temporal dynamics of B-ERD, and MRGS throughout the driving task and the significant emergence of FMT in coordination with both acceleration and braking behavior. Additionally, the power of MRGS was observed to change between early and late trials (stronger in the first 10 trials vs. the last 10 trials) in association with a significant decrease in trial duration.

These observations have several important ramifications. First, the TFR of dynamic motor related oscillatory activity (B-ERD and MRGS: well-characterized in artificial lab paradigms) raises the very real possibility of employing principled basic science methods to a complex and ecologically valid (and highly relevant to the real-world) experimental protocol. Second, by adopting an event-related design embedded in the realistic, albeit prototypical, driving scene, we can ascertain the temporal dynamics of neural oscillatory activity; most specifically, the dynamic interplay of FMT and motor cortex activity. If we hypothesize that FMT reflects surges of top-down cognitive control and motor cortex activity (B-ERD and MRGS) reflects implementation of task demands, then this dynamic interplay resolved in our experimental design may be seen to underly behavior. It is worth noting that while the spatial nodes of this cognitive control network might readily be resolved using other functional imaging modalities (fMRI: see Stanley et al., 2013) or even temporally-integrated MEG studies, our event-related approach additionally allows resolution of the temporal dynamics of each band-limited node in the driving task network.

The observation of a burst of FMT activity at the onset of acceleration and a sustained burst after the onset of braking implies increased demand for cognitive control over goal directed behavior (i.e., lower demands during acceleration, vs. higher demands when coordinating stopping the car at the target location directly before the intersection, when more precision is needed). Prior studies examining other cognitive control tasks have shown that FMT responses

originate in the dorsal anterior cingulate and adjacent medial prefrontal cortex (Domic-Siede et al., 2021; Van Veen & Carter, 2006; Womelsdorf et al., 2010) and it has been argued that FMT reflects the mechanism by which cognitive control is initiated, executed, and perhaps communicated across disparate brain regions (Cavanagh & Frank, 2014; Cooper et al., 2019; Eisma et al., 2021; Ishii et al., 2014; Nowak et al., 2018). However, most studies fail to establish the temporal dynamics of FMT interacting with imperative cues and cortical, as well as behavioral, responses (see Cavanagh & Frank, 2014; Eisma et al., 2021; Ishii et al., 2014).

Studies of simple motor tasks (finger tapping and button-pushing tasks) have not reported FMT responses, suggesting it may be invoked only in complex, coordinated and controlled motor behaviors. We suggest that, in contrast to simple button press tasks, even this prototypical but ecologically-valid simulated driving task creates a demand for more top-down cognitive control of motor behavior: more specifically, for ongoing updating and monitoring of speed and vehicle position when accelerating at the start of the trial and, even more so, when planning and managing braking with the goal of careful stopping at the next traffic light intersection (reflected in sustained FMT after brake onset). One prior MEG driving study revealed a significant increase in FMT during driving, but the authors' analysis approach, temporally-integrated over a 3-min window in which multiple motor actions occurred (Sakihara et al., 2014), limited the ability to associate FMT temporally with any of these specific motor actions. While Fort et al., used an event-related paradigm, similar to ours, their analysis was broadband and thus failed to appreciate frequency band specific changes in rhythmic activity (e.g., FMT, B-ERD, and MRGS). Our trials-based (event-related) paradigm, combined with frequency band selective analysis overcomes the limits of previous efforts by allowing for characterization of the neural correlates of realistic, complex motor activity in terms of brain regions, frequency bands and their dynamic temporal interplay.

Interestingly, post hoc analysis found an association between FMT power and a behavioral response of pedal onset time: FMT power at brake onset, in response to the red light at the upcoming intersection at the end of the trial, was associated with accelerator pedal onset time, in response to the green light at the start of the trial (linking FMT power to a behavioral response). However, we did not resolve two more intuitive associations: (i) FMT at accelerator onset associated with accelerator pedal onset time, and (ii) FMT power at brake onset associated with brake pedal onset time. The lack of observation of these more intuitively-anticipated relationships is mitigated by experimental design considerations: the relatively brief time to execute acceleration, and the less cognitively demanding task of executing this behavior, compared to the relatively protracted time and demands of the braking event (bringing the car to stop in response to changing traffic lights and an approaching intersection). Furthermore, the brake onset time represents a poor correlative variable since it is referenced to the green light cued accelerator onset at the start of the trial but does not account for speed during the trial.

One of the challenges implicit in our paradigm, or possibly any prolonged ecologically valid paradigm (or real life), is progressive

habituation/learning towards “auto pilot,” with both the positive and negative ramifications thereof. This learning/habituation effect was manifest as a significant decrease in trial duration over the course of 20 “repeats” and was associated with a progressive decrease in MRGS power. To our knowledge, this is the first demonstration of a significant within condition (early trials vs. late trials) change to MRGS power. Thus, this reduction in gamma power may reflect increased response certainty (with more gamma at the start when the trials were still novel), or reflect the learning process itself (with greater gamma at beginning trials while learning the new task: see Nowak et al., 2018 for a review of the functional significance of the role of MRGS activity in plasticity and learning). One prior study of repetitive finger movements saw MRGS activity maximally at the first movement of a sequence (Muthukumaraswamy, 2010). Another study of a bimanual finger tapping task involving congruent and incongruent cued trials showed that MRGS was reduced with increased contextual response certainty (Wiesman et al., 2021). Although it is not clear exactly what the change in gamma power reflects in the current study, it lends further support to prior arguments that MRGS reflects higher-level motor control or cognitive processing during movement in response to dynamic environmental demands (Nowak et al., 2018; Ulloa, 2022). While the current study did not reveal changes in FMT power over trials, prior work suggests that FMT and gamma oscillations may work together for motor learning by underpinning network-level plastic changes (Nowak et al., 2018). One recent study found that increasing theta-gamma phase amplitude coupling (PAC) via transcranial alternating current stimulation (tACS) to MI areas resulted in improved motor skill acquisition (Akkad et al., 2021). Exploring the theta-gamma PAC coupling during driving or other more complex motor tasks that require learning are exciting next steps for future research (Bramson et al., 2018; Dürschmid et al., 2014).

Finally, as hypothesized, beta desynchrony was also observed over the foot areas of the primary motor cortex MI during accelerator and brake pedal events and correlated with age, in line with previous work (Gaetz et al., 2010; Gaetz et al., 2020), despite the narrow age range of our sample. We did not see age correlate with gamma or theta frequencies as reported in other studies (Liu et al., 2014; Trevarrow et al., 2019), likely due to our narrow age-range. Furthermore, the beta modulation localized to more posterior areas of the superior parietal lobe was an unanticipated finding, as it is not usually observed on more basic motor tasks (i.e., visually-cued button-pressing tasks) (Heinrichs-Graham et al., 2018; Jurkiewicz et al., 2006). The superior parietal lobe is part of the dorsal-visual stream (the “where” pathway) known for processing location-in-space information, and has also been directly associated with visuo-motor integration and spatial working memory processing (Curtis, 2006; Proskovec et al., 2018). Both visuo-motor integration and spatial working memory are conceivably required for the performance of this driving task, particularly when monitoring speed and position when accelerating, and when planning and monitoring deceleration to stop at the intersection. More broadly, superior parietal areas have been identified as mediating top-down control of spatial attention (Corbetta et al., 2000).

In summary, these findings suggest that even this relatively simple prototypical simulated driving task can probe not only expected primary motor cortex responses (B-ERD) but also higher-level motor control (MRGS) and cognitive control (FMT) responses in relation to specific motor demands. With this paradigm, the level of complexity of the driving scene could be systematically increased by adding scenario features such as traffic, pedestrians, hazards, and distractions. Thus, building on these results, future studies may reveal additional frontal or other cognitive control neural responses related to driving behaviors that may be modulated by task difficulty or cognitive workload, distractions or both exogenous and endogenous confounds.

4.1 | Limitations

This study recruited a relatively young and small sample of adults, of which the majority was male, limiting the generalizability of the findings to the broader population. Future studies should explore these findings in a larger sample with broader age ranges to determine the consistency in the patterns. Signal to noise limitations prohibited us performing a trial-by-trial analysis of oscillatory power changes during the repeated trials of the paradigm. Nonetheless, we compared the first and second half of trials for changes in FMT, MRGS and B-ERD power. Again, future studies could examine changes in power over trials at a more granular level, perhaps with increases in SNR through optimized hardware, or through sliding window averaging algorithms. Furthermore, while we observed a positive association between B-ERD and age, no other rhythm appeared associated with age, likely due to the limited age range included in this study sample: a broader age range may likely reveal age related changes in MRGS and FMT power (Gaetz et al., 2013; Trevarrow et al., 2019). Of note, we also relied on average power which may not be the best metric for revealing variability with other factors, such as age. Future work can further examine the different properties of cortical oscillation responses, such as inter-trial coherence, in relation to task events and other factors. In addition, future studies should consider adding concurrent eye tracking measurement, to consider the relation to eye movements during the driving task.

4.2 | Conclusion

This study establishes an ecologically valid experimental paradigm, an event-related simulated driving task designed for use with frequency-specific differential beamformer spatial-filter analysis, allowing characterization of brain activity in space, time, and frequency. This proof-of-concept study first validated the utility of this paradigm for capturing primary motor cortex responses in foot areas relative to the onset of the gas and brake pedal, and further established its utility for measuring higher-level motor and frontal cognitive control responses in relation to specific driving events. Thus, this study adds to the field a more dynamic and ecologically relevant motor task, offering a path forward for better understanding of integrated cognitive-motor

processes and more real-world motor tasks, in typically developing and clinical populations.

ACKNOWLEDGMENTS

The authors thank all the participants for their time and effort. In addition, the authors would like to thank John Dell, Rachel Golemski, Erin Verzella, Peter Lam, Shivani Patel, and Na'Keisha Robinson, (RTs) for technical assistance, and Nicole Wen for assistance with recruitment and study visits. This study was supported in part by the National Institute of Health NIH-R21 5R21NS118410-02 (William Gaetz, Elizabeth A. Walshe, Flaura K. Winston, Timothy P. L. Roberts), the Children's Hospital of Philadelphia (CHOP) Foerderer Award, the Center for Child Injury Prevention Studies, the Center for Injury Research and Prevention at CHOP, and the Annenberg Public Policy Center at the University of Pennsylvania. The content is solely the responsibility of the authors and does not necessarily represent the official views of the listed funding sources. The listed funding sources had no role in the study design, collection, analysis, or interpretation of the data presented in this manuscript. We acknowledge in-kind support from Current Designs Inc. who supplied the driving simulation hardware, and Diagnostic Driving Inc. who provided the software platform for our custom-built driving task.

CONFLICT OF INTEREST

Author Winston has an intellectual property and financial interest in Diagnostic Driving, Inc. the company that provided the custom-built driving software in this study. The Children's Hospital of Philadelphia (CHOP) has an institutional financial interest in Diagnostic Driving, Inc. Dr. Winston serves as the chief scientific advisor of Diagnostic Driving, Inc. This potential conflict of interest is managed under a conflict of interest management plan from CHOP and the University of Pennsylvania whereby Dr. Winston has no interaction with participants and all analyses were reviewed and approved by outside consultant with no intellectual or financial interest (Dr. Seán Commins, a behavioral neuroscientist at Maynooth University, Ireland).

DATA AVAILABILITY STATEMENT

The magnetoencephalography data will be made available upon reasonable request to the corresponding author.

ORCID

Elizabeth A. Walshe  <https://orcid.org/0000-0002-0466-4272>

REFERENCES

- Akkad, H., Dupont-Hadwen, J., Frese, A., Tetkovic, I., Barrett, L., Bestmann, S., & Stagg, C. J. (2021). Increasing human motor skill acquisition by driving theta-gamma coupling. *eLife*, 10, e67355. <https://doi.org/10.7554/ELIFE.67355>
- Andersson, J., Smith, S., & Jenkinson, M. (2008). *FNIRT-FMRIB's non-linear image registration tool*. 14th Annual Meeting of the Organization for Human Brain Mapping.
- Anstey, K. J., Horswill, M. S., Wood, J. M., & Hatherly, C. (2012). The role of cognitive and visual abilities as predictors in the multifactorial model of driving safety. *Accident Analysis and Prevention*, 45, 766–774. <https://doi.org/10.1016/J.AAP.2011.10.006>
- Anstey, K. J., Wood, J., Lord, S., & Walker, J. G. (2005). Cognitive, sensory and physical factors enabling driving safety in older adults. *Clinical Psychology Review*, 25(1), 45–65. <https://doi.org/10.1016/J.CPR.2004.07.008>
- Apolinario, D., Magaldi, R. M., Busse, A. L., Lopes, L. d. C., Kasai, J. Y. T., & Satomi, E. (2009). Cognitive impairment and driving: A review of the literature. *Dementia & Neuropsychologia*, 3(4), 283–290. <https://doi.org/10.1590/S1980-57642009DN30400004>
- Balters, S., Baker, J. M., Geeseman, J. W., & Reiss, A. L. (2021). A methodological review of fNIRS in driving research: Relevance to the future of autonomous vehicles. *Frontiers in Human Neuroscience*, 15, 637589. <https://doi.org/10.3389/FNHUM.2021.637589>
- Balters, S., Sibi, S., Johns, M., Steinert, M., & Ju, W. (2017). *Learning-by-doing: using near infrared spectroscopy to detect habituation and adaptation in automated driving* (pp. 134–143). Proceedings of the 9th International Conference on Automotive User Interfaces and Interactive Vehicular Applications (ACM).
- Barratt, E. L., Francis, S. T., Morris, P. G., & Brookes, M. J. (2018). Mapping the topological organisation of beta oscillations in motor cortex using MEG. *NeuroImage*, 181, 831–844. <https://doi.org/10.1016/J.NEUROIMAGE.2018.06.041>
- Battaglia-Mayer, A., Caminiti, R., Lacquaniti, F., & Zago, M. (2003). Multiple levels of representation of reaching in the Parieto-frontal network. *Cerebral Cortex*, 13(10), 1009–1022. <https://doi.org/10.1093/CERCOR/13.10.1009>
- Baumann, M., & Krems, J. F. (2007). Situation awareness and driving: A cognitive model. In *Modelling driver behaviour in automotive environments. Critical issues in driver interactions with intelligent transport systems*, London: Springer. pp. 253–265. https://doi.org/10.1007/978-1-84628-618-6_14/COVER/
- Bramson, B., Jensen, O., Toni, X. I., & Roelofs, K. (2018). Cortical oscillatory mechanisms supporting the control of human social-emotional actions. *Journal of Neuroscience*, 38, 5739–5749. <https://doi.org/10.1523/JNEUROSCI.3382-17.2018>
- Calhoun, V., Pekar, J., & Pearson, G. (2004). Alcohol intoxication effects on simulated driving: Exploring alcohol-dose effects on brain activation using functional MRI. *Neuropsychopharmacology*, 29, 2097–2107. <https://doi.org/10.1038/sj.npp.1300543>
- Calhoun, V. D., & Pearson, G. D. (2012). A selective review of simulated driving studies: Combining naturalistic and hybrid paradigms, analysis approaches, and future directions. *NeuroImage*, 59(1), 25–35. <https://doi.org/10.1016/J.NEUROIMAGE.2011.06.037>
- Calhoun, V. D., Pekar, J. J., McGinty, V. B., Adali, T., Watson, T. D., & Pearson, G. D. (2002). Different activation dynamics in multiple neural systems during simulated driving. *Human Brain Mapping*, 16, 158–167. <https://doi.org/10.1002/hbm.10032>
- Cavanagh, J. F., & Frank, M. J. (2014). Frontal theta as a mechanism for cognitive control. In *Trends in cognitive sciences* (Vol. 18, pp. 414–421). Elsevier Ltd. <https://doi.org/10.1016/j.tics.2014.04.012>
- Cheyne, D., Bakhtazad, L., & Gaetz, W. (2006). Spatiotemporal mapping of cortical activity accompanying voluntary movements using an event-related beamforming approach. *Human Brain Mapping*, 27, 213–229.
- Cheyne, D., Bells, S., Ferrari, P., Gaetz, W., & Bostan, A. C. (2008). Self-paced movements induce high-frequency gamma oscillations in primary motor cortex. *NeuroImage*, 42(1), 332–342. <https://doi.org/10.1016/J.NEUROIMAGE.2008.04.178>
- Cheyne, D. O. (2013). MEG studies of sensorimotor rhythms: A review. *Experimental Neurology*, 245, 27–39. <https://doi.org/10.1016/j.expneurol.2012.08.030>
- Cohen, D. (1972). Magnetoencephalography: Detection of the brain's electrical activity with a superconducting magnetometer. *Science*, 175, 664–666.

- Cooper, P. S., Karayanidis, F., McKewen, M., McLellan-Hall, S., Wong, A. S. W., Skippen, P., & Cavanagh, J. F. (2019). Frontal theta predicts specific cognitive control-induced behavioural changes beyond general reaction time slowing. *NeuroImage*, 189, 130–140. <https://doi.org/10.1016/j.neuroimage.2019.01.022>.
- Corbetta, M., Kincade, J. M., Ollinger, J. M., Mcavoy, M. P., & Shulman, G. L. (2000). Voluntary orienting is dissociated from target detection in human posterior parietal cortex. *Nature Neuroscience*, 3(3), 292–297. <https://doi.org/10.1038/73009>
- Curtis, C. E. (2006). Prefrontal and parietal contributions to spatial working memory. *Neuroscience*, 139(1), 173–180. <https://doi.org/10.1016/J.NEUROSCIENCE.2005.04.070>
- Domic-Siede, M., Irani, M., Valdés, J., Perrone-Bertolotti, M., & Ossandón, T. (2021). Theta activity from frontopolar cortex, mid-cingulate cortex and anterior cingulate cortex shows different roles in cognitive planning performance. *NeuroImage*, 226, 117557. <https://doi.org/10.1016/J.NEUROIMAGE.2020.117557>
- Dürschmid, S., Quandt, F., Krämer, U. M., Hinrichs, H., Heinze, H. J., Schulz, R., Pannek, H., Chang, E. F., & Knight, R. T. (2014). Oscillatory dynamics track motor performance improvement in human cortex. *PLoS One*, 9(2), e89576. <https://doi.org/10.1371/journal.pone.0089576>
- Eisma, J., Rawls, E., Long, S., Mach, R., & Lamm, C. (2021). Frontal midline theta differentiates separate cognitive control strategies while still generalizing the need for cognitive control. *Scientific Reports*, 11(1), 14641. <https://doi.org/10.1038/s41598-021-94162-z>
- Fort, A., Martin, R., Jacquet-Andrieu, A., Combe-Pangaud, C., Foliot, G., Daligault, S., & Delpuech, C. (2010). Attentional demand and processing of relevant visual information during simulated driving: A MEG study. *Brain Research*, 1363, 117–127. <https://doi.org/10.1016/j.brainres.2010.09.094>
- Gaetz, W., Edgar, J. C., Wang, D. J., & Roberts, T. P. L. (2011). Relating MEG measured motor cortical oscillations to resting γ -aminobutyric acid (GABA) concentration. *NeuroImage*, 55(2), 616–621. <https://doi.org/10.1016/j.neuroimage.2010.12.077>
- Gaetz, W., Liu, C., Zhu, H., Bloy, L., & Roberts, T. P. L. (2013). Evidence for a motor gamma-band network governing response interference. *NeuroImage*, 74, 245–253. <https://doi.org/10.1016/j.neuroimage.2013.02.013>
- Gaetz, W., MacDonald, M., Cheyne, D., & Snead, O. C. (2010). Neuromagnetic imaging of movement-related cortical oscillations in children and adults: Age predicts post-movement beta rebound. *NeuroImage*, 51(2), 792–807. <https://doi.org/10.1016/j.neuroimage.2010.01.077>
- Gaetz, W., Rhodes, E., Bloy, L., Blaskey, L., Jackel, C. R., Brodtkin, E. S., Waldman, A., Embick, D., Hall, S., & Roberts, T. P. L. (2020). Evaluating motor cortical oscillations and age-related change in autism spectrum disorder. *NeuroImage*, 207, 116349. <https://doi.org/10.1016/J.NEUROIMAGE.2019.116349>
- Gharagozlou, F., Nasl Saraji, G., Mazloumi, A., Nahvi, A., Motie Nasrabadi, A., Rahimi Foroushani, A., Arab Kheradmand, A., Ashouri, M., & Samavati, M. (2015). Detecting driver mental fatigue based on EEG alpha power changes during simulated driving. *Iranian Journal of Public Health*, 44(12), 1693–1700.
- Haghani, M., Bliemer, M. C. J., Farooq, B., Kim, I., Li, Z., Oh, C., Shahhoseini, Z., & MacDougall, H. (2021). Applications of brain imaging methods in driving behaviour research. *Accident Analysis and Prevention*, 154, 106093. <https://doi.org/10.1016/j.aap.2021.106093>
- Hamandi, K., Singh, K. D., & Muthukumaraswamy, S. (2011). Reduced movement-related β desynchronization in juvenile myoclonic epilepsy: a MEG study of task specific cortical modulation. *Clinical Neurophysiology: Official Journal of the International Federation of Clinical Neurophysiology*, 122(11), 2128–2138. <https://doi.org/10.1016/J.CLINPH.2011.04.017>
- Hämäläinen, M., Hari, R., Ilmoniemi, R., Knuutila, J., & Lounasmaa, O. (1993). Magnetoencephalography: Theory, instrumentation and applications to the noninvasive study of human brain function. *Reviews of Modern Physics*, 65, 413–497.
- Heinrichs-Graham, E., McDermott, T. J., Mills, M. S., Wiesman, A. I., Wang, Y. P., Stephen, J. M., Calhoun, V. D., & Wilson, T. W. (2018). The lifespan trajectory of neural oscillatory activity in the motor system. *Developmental Cognitive Neuroscience*, 30, 159–168. <https://doi.org/10.1016/J.DCN.2018.02.013>
- Heinrichs-Graham, E., & Wilson, T. W. (2015). Coding complexity in the human motor circuit. *Human Brain Mapping*, 36, 5155–5167.
- Heinrichs-Graham, E., & Wilson, T. W. (2016). Is an absolute level of cortical beta suppression required for proper movement? Magnetoencephalographic evidence from healthy aging. *NeuroImage*, 134, 514–521.
- Heinrichs-Graham, E., Wilson, T. W., Santamaria, P. M., Heithoff, S. K., Torres-Russotto, D., Hutter-Saunders, J. A., Estes, K. A., Meza, J. L., & Mosley, R. L. (2014). Neuromagnetic evidence of abnormal movement-related beta desynchronization in Parkinson's disease. *Cereb. Cortex*, 24, 2669–2678.
- Ishii, R., Canuet, L., Ishihara, T., Aoki, Y., Ikeda, S., Hata, M., Katsimichas, T., Gunji, A., Takahashi, H., Nakahachi, T., Iwase, M., & Takeda, M. (2014). Frontal midline theta rhythm and gamma power changes during focused attention on mental calculation: An MEG beamformer analysis. *Frontiers in Human Neuroscience*, 8(6), 1–10. <https://doi.org/10.3389/fnhum.2014.00406>
- Jurkiewicz, M. T., Gaetz, W. C., Bostan, A. C., & Cheyne, D. (2006). Post-movement beta rebound is generated in motor cortex: Evidence from neuromagnetic recordings. *NeuroImage*, 32(3), 1281–1289. <https://doi.org/10.1016/J.NEUROIMAGE.2006.06.005>
- Kan, K., Schweizer, T. A., Tam, F., & Graham, S. J. (2013). Methodology for functional MRI of simulated driving. *Medical Physics*, 40, 012301. <https://doi.org/10.1118/1.4769107>
- Li, G., & Chung, W. Y. (2022). Electroencephalogram-based approaches for driver drowsiness detection and management: A review. *Sensors*, 22(3), 1100. <https://doi.org/10.3390/S22031100>
- Liu, Z., Woltering, S., & Lewis, M. D. (2014). Developmental change in EEG theta activity in the medial prefrontal cortex during response control. *NeuroImage*, 85, 873–887. <https://doi.org/10.1016/j.neuroimage.2013.08.054>
- Muthukumaraswamy, S. D. (2010). Functional properties of human primary motor cortex gamma oscillations. *Journal of Neurophysiology*, 104(5), 2873–2885. <https://doi.org/10.1152/JN.00607.2010>
- Nichols, T. E., & Holmes, A. P. (2002). Nonparametric permutation tests for functional neuroimaging: a primer with examples. *Human Brain Mapping*, 1(1), 1–25. <https://doi.org/10.1002/HBM.10582>
- Nowak, M., Zich, C., & Stagg, C. J. (2018). Motor cortical gamma oscillations: What have we learnt and where are we headed? *Current Behavioral Neuroscience Reports*, 5(2), 136–142. <https://doi.org/10.1007/S40473-018-0151-Z>
- Pfurtscheller, G., Graftmann, B., Huggins, J. E., Levine, S. P., & Schuh, L. A. (2003). Spatiotemporal patterns of beta desynchronization and gamma synchronization in corticographic data during self-paced movement. *Clinical Neurophysiology*, 114(7), 1226–1236. [https://doi.org/10.1016/S1388-2457\(03\)00067-1](https://doi.org/10.1016/S1388-2457(03)00067-1)
- Proskovec, A. L., Wiesman, A. I., Heinrichs-Graham, E., & Wilson, T. W. (2018). Beta oscillatory dynamics in the prefrontal and superior temporal cortices predict spatial working memory performance. *Scientific Reports*, 8(1), 1–13. <https://doi.org/10.1038/s41598-018-26863-x>
- Rossiter, H. E., Davis, E. M., Clark, E. V., Boudrias, M. H., & Ward, N. S. (2014). Beta oscillations reflect changes in motor cortex inhibition in healthy ageing. *NeuroImage*, 91, 360–365. <https://doi.org/10.1016/J.NEUROIMAGE.2014.01.012>
- Sakihara, K., Hirata, M., Ebe, K., Kimura, K., Yi Ryu, S., Kono, Y., Muto, N., Yoshioka, M., Yoshimine, T., & Yorifuji, S. (2014). Cerebral oscillatory activity during simulated driving using MEG. *Frontiers in Human Neuroscience*, 8(December), 1–9. <https://doi.org/10.3389/fnhum.2014.00975>

- Schier, M. A. (2000). Changes in EEG alpha power during simulated driving: A demonstration. *International Journal of Psychophysiology*, 37(2), 155–162. [https://doi.org/10.1016/S0167-8760\(00\)00079-9](https://doi.org/10.1016/S0167-8760(00)00079-9)
- Schweizer, T. A., Kan, K., Hung, Y., Tam, F., Naglie, G., & Graham, S. (2013). Brain activity during driving with distraction: An immersive fMRI study. *Frontiers in Human Neuroscience*, 7, 53. <https://doi.org/10.3389/fnhum.2013.00053>
- Spiers, H. J., & Maguire, E. A. (2007). Neural substrates of driving behaviour. *NeuroImage*, 36(1), 245–255. <https://doi.org/10.1016/j.neuroimage.2007.02.032>
- Stanley, M. L., Moussa, M. N., Paolini, B. M., Lyday, R. G., Burdette, J. H., & Laurienti, P. J. (2013). Defining nodes in complex brain networks. *Frontiers in Computational Neuroscience*, 7, 169. <https://doi.org/10.3389/FNCOM.2013.00169/ABSTRACT>
- Trevarrow, M. P., Kurz, M. J., McDermott, T. J., Wiesman, A. I., Mills, M. S., Wang, Y. P., Calhoun, V. D., Stephen, J. M., & Wilson, T. W. (2019). The developmental trajectory of sensorimotor cortical oscillations. *NeuroImage*, 184, 455–461. <https://doi.org/10.1016/J.NEUROIMAGE.2018.09.018>
- Ulloa, J. L. (2022). The control of movements via motor gamma oscillations. *Frontiers in Human Neuroscience*, 15, 837. <https://doi.org/10.3389/FNHUM.2021.787157/BIBTEX>
- Van Veen, V., & Carter, C. S. (2006). Conflict and cognitive control in the brain. *Current Directions in Psychological Science*, 15(5), 237–240. <https://doi.org/10.1111/J.1467-8721.2006.00443.X>
- van Wijk, B. C. M., Beek, P. J., & Daffertshofer, A. (2012). Neural synchrony within the motor system: What have we learned so far? *Frontiers in Human Neuroscience*, 6, 252. <https://doi.org/10.3389/FNHUM.2012.00252>
- Vrba, J., & Robinson, S. E. (2001). Signal processing in magnetoencephalography. *Methods*, 25(2), 249–271. <https://doi.org/10.1006/meth.2001.1238>
- Walter, H., Vetter, S., Grothe, J., Wunderlich, A. P., Hahn, S., & Spitzer, M. (2001). The neural correlates of driving and co-driving. *NeuroImage*, 13(6), 1277. [https://doi.org/10.1016/S1053-8119\(01\)92591-1](https://doi.org/10.1016/S1053-8119(01)92591-1)
- Wenderoth, N., Toni, I., Bedeleem, S., Debaere, F., & Swinnen, S. P. (2006). Information processing in human parieto-frontal circuits during goal-directed bimanual movements. *NeuroImage*, 31(1), 264–278. <https://doi.org/10.1016/J.NEUROIMAGE.2005.11.033>
- Wiesman, A. I., Christopher-Hayes, N. J., Eastman, J. A., Heinrichs-Graham, E., & Wilson, T. W. (2021). Response certainty during bimanual movements reduces gamma oscillations in primary motor cortex. *NeuroImage*, 224, 117448. <https://doi.org/10.1016/J.NEUROIMAGE.2020.117448>
- Wiesman, A. I., Koshy, S. M., Heinrichs-Graham, E., & Wilson, T. W. (2020). Beta and gamma oscillations index cognitive interference effects across a distributed motor network. *NeuroImage*, 213, 116747. <https://doi.org/10.1016/j.neuroimage.2020.116747>
- Wilson, T. W., Slason, E., Asherin, R., Kronberg, E., Reite, M. L., Teale, P. D., & Rojas, D. C. (2010). An extended motor network generates beta and gamma oscillatory perturbations during development. *Brain and Cognition*, 73(2), 75–84. <https://doi.org/10.1016/J.BANDC.2010.03.001>
- Wilson, T. W., Slason, E., Asherin, R., Kronberg, E., Teale, P. D., Reite, M. L., & Rojas, D. C. (2011). Abnormal gamma and beta MEG activity during finger movements in early-onset psychosis. *Developmental Neuropsychology*, 36(5), 596–613. <https://doi.org/10.1080/87565641.2011.555573>
- Womelsdorf, T., Johnston, K., Vinck, M., & Everling, S. (2010). Theta-activity in anterior cingulate cortex predicts task rules and their adjustments following errors. *Proceedings of the National Academy of Sciences of the United States of America*, 107(11), 5248–5253. https://doi.org/10.1073/PNAS.0906194107/SUPPL_FILE/PNAS.200906194SI.PDF
- Xu, G., Zhang, M., Wang, Y., Liu, Z., Huo, C., Li, Z., & Huo, M. (2017). Functional connectivity analysis of distracted drivers based on the wavelet phase coherence of functional near-infrared spectroscopy signals. *PLOS One*, 12(11), e0188329. <https://doi.org/10.1371/journal.pone.0188329>
- Yuen, N. H., Tam, F., Churchill, N. W., Schweizer, T. A., & Graham, S. J. (2021). Driving with distraction: Measuring brain activity and oculomotor behavior using fMRI and eye-tracking. *Frontiers in Human Neuroscience*, 15, 659040. <https://doi.org/10.3389/fnhum.2021.659040>
- Zhao, C., Zhao, M., Liu, J., & Zheng, C. (2012). Electroencephalogram and electrocardiograph assessment of mental fatigue in a driving simulator. *Accident; Analysis and Prevention*, 45, 83–90. <https://doi.org/10.1016/j.aap.2011.11.019>

How to cite this article: Walshe, E. A., Roberts, T. P. L., Ward McIntosh, C., Winston, F. K., Romer, D., & Gaetz, W. (2023). An event-based magnetoencephalography study of simulated driving: Establishing a novel paradigm to probe the dynamic interplay of executive and motor function. *Human Brain Mapping*, 44(5), 2109–2121. <https://doi.org/10.1002/hbm.26197>